THE JOURNAL OF BIOLOGICAL CHEMISTRY VOL. 290, NO. 13, pp. 8644–8655, March 27, 2015

Urotensin-II Receptor Stimulation of Cardiac L-type Ca^{2+} Channels Requires the $\beta\gamma$ Subunits of $G_{i/o}$-protein and Phosphatidylinositol 3-Kinase-dependent Protein Kinase C β1 Isoform*

Received for publication, September 29, 2014, and in revised form, February 2, 2015 Published, JBC Papers in Press, February 12, 2015, DOI 10.1074/jbc.M114.615021

Yuan Zhang[‡§1], Jiaoqian Ying[‡¶1], Dongsheng Jiang[‡‖1], Zhigang Chang[‡], Hua Li[‡], Guoqiang Zhang[¶], Shan Gong[‡], Xinghong Jiang[‡], and Jin Tao[‡2]**

*From the [‡]Department of Physiology and Neurobiology, Medical College of Soochow University, Suzhou 215123, China, [§]Department of Geriatrics and Institute of Neuroscience, the Second Affiliated Hospital of Soochow University, Suzhou 215004, China, [¶]Department of Emergency Medicine, China-Japan Friendship Hospital, Beijing 100029, China, [‖]Department of Dermatology and Allergic Diseases, University of Ulm, Ulm 89081, Germany, and **National Shanghai Center for New Drug Safety Evaluation and Research, Shanghai 201203, China*

Background: Regulation of L-type Ca^{2+} channels has important roles in determining the electrical properties of cardiomyocytes.
Results: U-II potentiates $I_{Ca,L}$ via U-IIR that couples to the PI3K-dependent PKCβ_1 isoform.
Conclusion: U-IIR stimulation of $I_{Ca,L}$ contributes to the increase in the amplitude of sarcomere shortening.
Significance: Regulation of $I_{Ca,L}$ by U-IIR plays important roles in cardiovascular actions including cardiac positive inotropic effects and increasing cardiac output.

Recent studies have demonstrated that urotensin-II (U-II) plays important roles in cardiovascular actions including cardiac positive inotropic effects and increasing cardiac output. However, the mechanisms underlying these effects of U-II in cardiomyocytes still remain unknown. We show by electrophysiological studies that U-II dose-dependently potentiates L-type Ca^{2+} currents ($I_{Ca,L}$) in adult rat ventricular myocytes. This effect was U-II receptor (U-IIR)-dependent and was associated with a depolarizing shift in the voltage dependence of inactivation. Intracellular application of guanosine-5′-*O*-(2-thiodiphosphate) and pertussis toxin pretreatment both abolished the stimulatory effects of U-II. Dialysis of cells with the QEHA peptide, but not scrambled peptide SKEE, blocked the U-II-induced response. The phosphatidylinositol 3-kinase (PI3K) inhibitor wortmannin as well as the class I PI3K antagonist CH132799 blocked the U-II-induced $I_{Ca,L}$ response. Protein kinase C antagonists calphostin C and chelerythrine chloride as well as dialysis of cells with 1,2bis(2aminophenoxy)-ethane*N,N,N′,N′*-tetraacetic acid abolished the U-II-induced responses, whereas PKCα inhibition or PKA blockade had no effect. Exposure of ventricular myocytes to U-II markedly increased membrane PKCβ_1 expression, whereas inhibition of PKCβ_1 pharmacologically or by shRNA targeting abolished the U-II-induced $I_{Ca,L}$ response. Functionally, we observed a significant increase in the amplitude of sarcomere shortening induced by U-II; blockade of U-IIR as well as PKCβ inhibition abolished this effect, whereas Bay K8644 mimicked the U-II response. Taken together, our results indicate that U-II potentiates $I_{Ca,L}$ through the $\beta\gamma$ subunits of $G_{i/o}$-protein and downstream activation of the class I PI3K-dependent PKCβ_1 isoform. This occurred via the activation of U-IIR and contributes to the positive inotropic effect on cardiomyocytes.

Urotensin-II (U-II)[3] is a cyclic peptide first identified in the goby urophysis, an endocrine organ homologous in structure to the mammalian hypothalamoneurohypophysial axis (1). Following the cloning of carp U-II cDNAs (2), U-II has since been cloned from additional vertebrates including humans (3). The orphan G-protein-coupled receptor GPR14 (3), subsequently redesignated the urotensin-II receptor (U-IIR) (4), has been identified as the endogenous receptor for U-II. Consistent with the broad distribution of U-IIR in the central nervous system (CNS) and peripheral organs (2, 5), U-II exerts a large array of behavioral effects and regulates a variety of physiological processes including stimulation of prolactin and thyrotropin release (6), modulation of immune function (7), enhancement

* This work was supported by National Natural Science Foundation of China Grants 81171056, 31271258, 81200852, and 81371229; National Natural Science Foundation of China-CNRS Joint Program Grant 81311130114; Natural Science Funding of Jiangsu Province Grant BK2011293; Natural Science Funding for Colleges and Universities in Jiangsu Province Grant 12KJB320010; Scientific Research Foundation for the Returned Overseas Chinese Scholars of State Education Ministry (to J. T.); Dong-Wu Scholar Funding of Soochow University (to J. T.); National University Student Innovation Programs (to Hong Jin); and a project funded by the Priority Academic Program Development of Jiangsu Higher Education Institutions.
[1] These authors contributed equally to this work.
[2] To whom correspondence should be addressed: Dept. of Physiology and Neurobiology, Medical College of Soochow University, 199 Ren-Ai Rd., Suzhou 215123, China. Tel./Fax: 86-512-65880126; E-mail: taoj@suda.edu.cn.

[3] The abbreviations used are: U-II, urotensin-II; U-IIR, urotensin-II receptor; $I_{Ca,L}$, L-type Ca^{2+} current; PTX, pertussis toxin; G$\beta\gamma$, G-protein $\beta\gamma$ subunit; GDP-β-S, guanosine-5′-*O*-(2-thiodiphosphate); BAPTA, 1,2bis(2aminophenoxy)ethane*N,N,N′,N′*-tetraacetic acid; dn-BAPTA, 5,5′-dinitro-BAPTA; HBDDE, 2,2′,3,3′,4,4′-hexahydroxy-1,1′-biphenyl-6,6′-dimethanol dimethyl ether; NC, negative control.

of rapid eye movement sleep duration (8), and energy balance (5). In the cardiovascular system, particularly in the heart, both U-II and the U-IIR are endogenously expressed (2), suggesting that U-II may be an endogenous modulator of mammalian cardiovascular function. Indeed, U-II has been shown to exert potent contractile force of cardiac muscle *in vitro* (9). U-II has also been reported to increase cardiac output in healthy humans and in patients with heart failure (10–12) independently of serotonin or β-adrenergic receptors (9). In addition, U-II has a positive inotropic effect and improves cardiac performance in rats with congestive heart failure as indicated by increases in left ventricular maximum dP/dT (an index of myocardial contractility) and left ventricular fractional shortening (2, 5, 13, 14). However, the mechanisms underlying these effects of U-II in cardiomyocytes remain unknown.

L-type Ca^{2+} channels are voltage-dependent channels that open in response to membrane depolarization, permitting entry of Ca^{2+} into the cell (15). Ca^{2+} entry through L-type Ca^{2+} channels is critical in the control of excitation-contraction coupling of cardiac, skeletal, and smooth muscle cells and contributes to physiological frequency regulation in the sinus node (16–18). Furthermore, the L-type Ca^{2+} channel is important for determining the duration of the plateau phase of the action potential and refractoriness. It is also involved in Ca^{2+} release from the sarcoplasmic reticulum, raising the free intracellular Ca^{2+} concentration and allowing cell contraction (18–21). Importantly, these channels are modulated by a variety of hormones and transmitters operating via G-protein-coupled receptors and second messengers (22), thereby profoundly affecting target tissue functions.

However, little is known about the mechanism(s) involved in the effect of U-II on L-type Ca^{2+} channels in the heart. Therefore, the present study sought to elucidate the signaling pathways implicated in L-type Ca^{2+} channel modulation by U-II in adult rat ventricular myocytes.

EXPERIMENTAL PROCEDURES

Pharmacological Agents—All the chemicals were obtained from Sigma-Aldrich unless otherwise stated. QEHA and SKEE peptides (23) were synthesized by GenScript Corp. βIV5-3 (24) and βIIV5-3 (24, 25) were synthesized by American Peptide, Inc. Stock solutions of U-II, GDP-β-S, pertussis toxin (PTX), cholera toxin, chelerythrine chloride, Ro 31-8220, BAPTA, and dn-BAPTA were prepared in distilled deionized water. Stock solutions of wortmannin, calphostin C, KT-5720, forskolin, LY333531, CH5132799, Bay K8644, HBDDE, and palosuran were prepared in dimethyl sulfoxide (DMSO). The final concentration of DMSO in the bath solution was less than 0.01% and had no functional effects on L-type Ca^{2+} channel currents (data not shown).

Isolation of Ventricular Myocytes—All the procedures and protocols conformed to the *Guide for Care and Use of Laboratory Animals* published by the National Institutes of Health, and the local institutional ethical committee approved the study. Left ventricular myocytes were enzymatically dissociated from rat hearts using a modified method described previously (26, 27). Briefly, male Sprague-Dawley rats (200–300 g) were injected with heparin (1000 IU intraperitoneally) and then euthanized in a CO_2 chamber. The heart was dissected out and transferred to ice-cold Tyrode's solution. The aorta was cannulated, and the heart was mounted on a Langendorff apparatus and perfused with prewarmed (37 °C) and oxygenated Tyrode's solution containing protease type XIV and collagenase type I for 12 min until the heart was flaccid. The left ventricles were dissected out, cut into small pieces, and gently bathed in Tyrode's solution. Isolated cells were filtered and maintained in oxygenated Kraft-Brühe (KB) solution. Cells with a rod shape and clear cross-striation were used for experiments. For short hairpin RNA (shRNA) knockdown experiments, primary cultures of adult rat ventricular myocytes were cultured in serum-free Medium 199 (Invitrogen) containing taurine (5 mM), creatine (5 mM), L-carnitine (5 mM), and sodium bicarbonate (26 mM) and plated in 24-well plates onto 12-mm glass coverslips coated with matrigel (BD Biosciences). All the media used for the cell culture contained 50 IU penicillin and 50 μg/ml streptomycin, and the cells were incubated under sterile conditions at 5% CO_2 and 37 °C.

Reverse Transcription-PCR (RT-PCR)—Total RNA was extracted from rat ventricular myocytes using the RNeasy kit (Qiagen) according to the manufacturer's instructions. Reverse transcription was performed using SuperScript™ II (Invitrogen) as described previously (23, 28, 29). Control reactions without reverse transcriptase were performed for determining contamination, if any, in the samples. The primer sequences used in this study were as follows: U-IIR: sense, 5′-cagctcccctgaaagaccttg-3′; antisense, 5′-acaatgctggtcccaaagag-3′; and GAPDH: sense, 5′-atgggaagctggtcatcaac-3′; antisense, 5′-ggagacaacctggtcctcag-3′.

Western Blotting—Western blot analysis was performed as described previously (30, 31). Briefly, total cellular protein was extracted from rat ventricular myocytes using homogenization buffer. Equivalent amounts of proteins (20 μg) were separated by 7.5% SDS-PAGE and transferred onto polyvinylidene difluoride (PVDF) membranes (Amersham Biosciences). Membranes were blocked using 5% (w/v) skimmed milk in phosphate-buffered saline (PBS) for 1 h at room temperature. Membranes were then probed using the following primary antibodies: rabbit anti-U-IIR (1:600; Santa Cruz Biotechnology), rabbit anti-G_q (1:1000; Santa Cruz Biotechnology), rabbit anti-phosphorylated Akt (1:500; Cell Signaling Technology), rabbit anti-total Akt (1:500; Cell Signaling Technology), rabbit anti-PKCα (1:600; Santa Cruz Biotechnology), mouse anti-PKCβ_1 (1:600; Sigma), rabbit anti-PKCβ_2 (1:1000; Sigma), rabbit anti-PKC$_\gamma$ (1:1000; Santa Cruz Biotechnology), and rabbit anti-GAPDH (1:2000; Cell Signaling Technology). After washing in Tris-buffered saline (TBS) and Tween 20 (TBS-T), the membranes were incubated with horseradish peroxidase-conjugated anti-rabbit or anti-mouse IgG (1:10,000) for 2 h at room temperature. Chemiluminescence signals were generated using a SuperSignal West Pico trial kit (Pierce). Quantification software (Bio-Rad) was used for background subtraction and for analyzing the immunoblotting data.

Protein Kinase A (PKA) Activity Assay—PKA activity in homogenates from isolated cardiomyocytes was determined by enzyme-linked immunosorbent assay (ELISA; Promega, Madison, WI) according to the manufacturer's instructions. Briefly,

the cells were pretreated with either vehicle or KT-5720 for 30 min followed by treatment with either vehicle (0.1% DMSO) or forskolin for 15 min. The cells were washed with ice-cold PBS, placed on ice, and incubated with 200 μl of lysis buffer. After a 10-min incubation on ice, the cells were transferred to microcentrifuge tubes. Cell lysates were centrifuged for 15 min, and aliquots of the supernatants containing 0.2 μg of protein were assayed for PKA activity. The activity is expressed as relative light units^{-1}/amount of protein.

Determination of PKC Activity—The cells were pretreated with either vehicle or calphostin C for 30 min at 37 °C followed by treatment with either vehicle or U-II for 15 min. Cells were resuspended in 50 μl of buffer A (20 μM Tris, 2 μM EDTA, 0.5 μM EGTA, and 1 μM PMSF, pH 7.4) containing 50 μM 2-mercaptoethanol and 25 μl of 10% Nonidet P-40 followed by sonication for 45 s. The cell lysates were centrifuged at 100,000 $\times$ *g* for 1 h and stored at −20 °C. PKC activity was determined using the PepTag PKC assay kit (Promega) according to the manufacturer's instructions.

Phosphatidylinositol 3-Kinase (PI3K) Activity Assay—Cells were stimulated with or without U-II (0.1 μM) for 15 min. After stimulation, PI3K activity was determined using a phosphatidylinositol 3-kinase activity ELISA kit according to the manufacturer's instructions (Tian-Ao Biotechnology). The absorbance of samples was measured at 450 nm with an EL 340 Bio Kinetic Reader (Bio-Tek Instruments).

Adenovirus Transduction—Three shRNAs targeting the sequence of PKCβ_1 (GenBank^{TM} accession number NM_012713.3) or G_q (GenBank accession number Y17161.1) were designed, and the best knockdown effects of shRNA for G_q (5′-CGCGGAGAUCGAGAAACAG-3′) and PKCβ_1 (5′-CACAUCCAACAAGUUGGCCGUUUCA-3′) were selected for subsequent experiments. Additional scrambled sequences also were designed as negative controls (NCs) (G_q, AGAUGAGAGAGCACACCGG; PKCβ_1, GUACUCACCUGACUCAUCAUGCAAG). The recombinant adenoviruses containing G_q shRNA (Ad-G_q-shRNA) or PKCβ_1 shRNA (Ad-PKCβ_1-shRNA) were packaged by GeneChem (Shanghai, China) using the pAdeasy system with pAdtrack-CMV-GFP as a shuttle vector and pAdeasy-1 as an adenoviral backbone. The virus was purified on two consecutive cesium chloride gradients, dialyzed, and titered. The titer of viral preparations used in the studies ranged from 10^9 to 10^{10} pfu/ml. Forty-eight hours after infection, cells showing green fluorescence under an inverted fluorescence microscope (Ti-2000, Nikon) were subjected to whole-cell patch clamp analysis. RNAi efficacy on G_q or PKCβ_1 expression was analyzed by Western blot analysis.

Measurement of Myocyte Contraction—Cell shortening of ventricular myocytes was assessed by a video-based edge detection system (IonOptix Corp.). The cells were placed in a perfusion chamber mounted on the stage of an inverted microscope (Zeiss IM). The cells were field-stimulated with 20% suprathreshold voltage at a frequency of 0.5 Hz with a pair of platinum electrodes. The myocyte being studied was displayed on the computer monitor with the help of an IonOptix MyoCam charge-coupled device camera, which was attached to the sidearm of the microscope. SoftEdge acquisition software (IonOptix Corp.) captured and converted the changes in sarcomere length to digital signals. Only rod-shaped myocytes with clear edges were selected for experiments. Signals were recorded when steady-state contraction was reached in each experimental medium.

Electrophysiology and Data Analysis—Whole cell patch clamp electrophysiology was used to measure the L-type Ca^{2+} currents ($I_{Ca,L}$) in rat ventricular myocytes. Cells were placed in a recording dish and perfused with a bath solution containing 140 mM tetraethylammonium chloride, 2 mM $CaCl_2$, 0.5 mM $MgCl_2$, 5.5 mM glucose, 5 mM CsCl, and 10 mM HEPES, pH 7.35 with CsOH. Recordings were performed at room temperature (22–24 °C) using a MultiClamp 700B amplifier (Molecular Devices). Recording pipettes (World Precision Instruments) had 2–3-megaohm resistance when filled with internal solution containing 110 mM CsCl, 4 mM Mg-ATP, 0.3 mM Na_2-GTP, 10 mM EGTA, and 25 mM HEPES, pH 7.3 with CsOH. pClamp 10.2 was used to acquire and analyze all data. $I_{Ca,L}$ were recorded in voltage clamp mode, and signals were filtered at 1 kHz using a low pass Bessel filter and digitized at 5 kHz. Series resistance and capacitance readings were taken directly from the amplifier after electronic subtraction of capacitive transients. Series resistance was compensated to the maximal extent (at least 75%). Current traces were corrected using on-line P/6 trace subtraction. In experiments in which cells were dialyzed with compounds or peptides, current measurements were started at least 5 min after breaking the patch. $I_{Ca,L}$ were measured at their peak amplitude within the 200-ms test pulse and used to determine the percentage of $I_{Ca,L}$ increase. Concentration-response curves were fitted by the following sigmoidal Hill equation: $I/I_{control} = 1/(1 + 10^{(\log(IC50) - X)n_H})$ where X is the decadic logarithm of the concentration used, IC_{50} is the concentration at which the half-maximum effect occurs, and n_H is the Hill coefficient. Activation data were fitted by the following modified Boltzmann equation: $G/G_{max} = 1/\{1 + \exp[-(V_{half} - V_m)/k]\}$ where G_{max} is the fitted maximal conductance, V_{half} is the membrane potential for half-activation, and k is the slope factor. Steady-state inactivation of I_A was fitted with the following negative Boltzmann equation: $I/I_{max} = 1/\{1 + \exp[-(V_{half} - V_m)/k]\}$ where I_{max} is maximal current, V_{half} is the membrane potential for half-inactivation, and k is the slope factor. Summary data are expressed as mean ± S.E. GraphPad Prism 5.0 was used to analyze the data. Statistical significance was determined using Student's t test when two groups were compared and one-way analysis of variance with a post hoc Bonferroni test when three or more groups were compared. Results were considered statistically significant at a p value of <0.05.

RESULTS

U-II Enhances $I_{Ca,L}$—Whole-cell currents were elicited by a 200-ms stepping voltage from a holding potential of −60 to 0 mV. These currents can be blocked by nicardipine (5 μM), a specific L-type Ca^{2+} channel blocker (data not shown). Addition of U-II (0.1 μM) to the bath caused a significant increase in peak $I_{Ca,L}$ to 28.3% of the basal level (n = 8; Fig. 1, *A* and *B*). Following removal of U-II, the amplitude of $I_{Ca,L}$ recovered partially within 5 min (Fig. 1, *B* and *C*). Further examination of the U-II effect demonstrated that U-II increased $I_{Ca,L}$ in a concen-

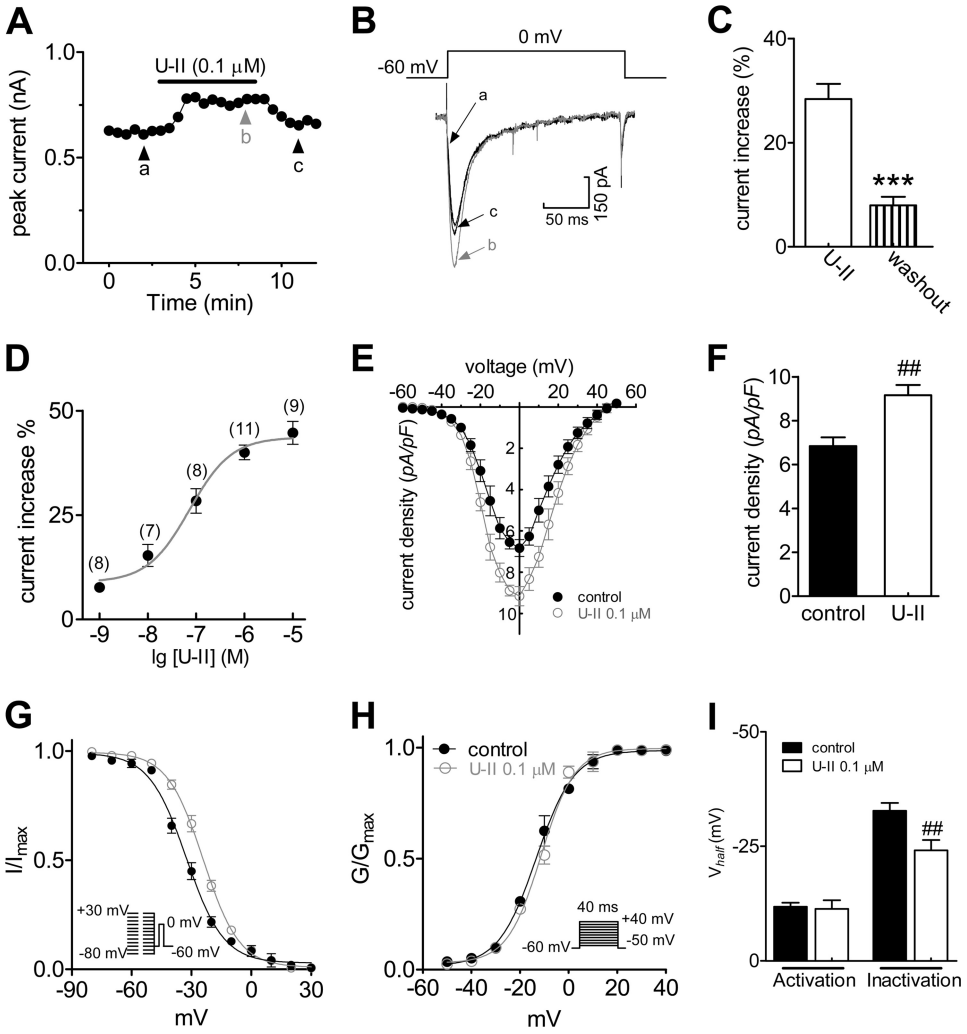

FIGURE 1. **U-II stimulates L-type Ca^{2+} channels in adult rat ventricular myocytes.** *A*, time course of changes in $I_{Ca,L}$ amplitude mediated by 0.1 μM U-II. *Letters* (*a*–*c*) indicate which points were used for sample traces. *B* and *C*, representative traces and summary data of $I_{Ca,L}$ under control conditions (*a*), during exposure to 0.1 μM U-II (*b*), and during washout (*c*) ($n = 8$). $I_{Ca,L}$ were elicited by a 200-ms-long depolarizing step pulse from the holding potential of −60 to 0 mV. *D*, dose response of U-II on the stimulation of $I_{Ca,L}$. The *dotted line* represents the line of best fit to the sigmoidal Hill equation. The number of cells tested at each concentration of U-II are indicated in *parentheses*. *E*, current-voltage plot showing the current density of $I_{Ca,L}$ *versus* test voltage recorded before and after treatment with 0.1 μM U-II ($n = 12$). *F*, summary of results showing the current density of $I_{Ca,L}$ at 0 mV as indicated in *E*. *G*–*I*, U-II did not significantly alter the steady-state activation curve of L-type Ca^{2+} channels (*H*; $n = 9$) but caused a rightward shift of the steady-state inactivation curve (*G*; $n = 11$). To determine the steady-state inactivation, $I_{Ca,L}$ was evoked by a 100-ms test pulse to 0 mV after the 3-s conditioning pulses ranging from −80 to +30 mV with 10-mV increments. To determine the voltage dependence of activation, tail currents were elicited by repolarization to −60 mV after 40-ms test pulses from −50 to +40 mV in increments of 10 mV. *I*, summary of results showing the effects of 0.1 μM U-II on V_{half} of the activation and inactivation curves. ***, $p < 0.001$ *versus* 0.1 μM U-II; ##, $p < 0.01$ *versus* control. *Error bars* represent S.E. *pF*, picofarad.

tration-dependent manner (Fig. 1*D*). The relationship between U-II concentration and the degree of increase observed is described by a logistic equation where the concentration of U-II producing half-maximal increase (IC_{50}) is 62.7 nM, the apparent Hill coefficient is 0.86, and the maximal stimulatory effect is 45.2 ± 1.8% ($n = 9$; Fig. 1*D*).

Next, we determined whether the biophysical properties of $I_{Ca,L}$ were affected by U-II. A current-voltage curve was evoked by a series of depolarizing pulses from a holding potential of −60 mV to test potentials between −60 and +50 mV. Population data showed that 0.1 μM U-II significantly down-shifted the current-voltage curve ($n = 12$; Fig. 1*E*), and at 0 mV, the current density increased from 6.8 ± 0.7 to 9.1 ± 0.6 pA/picofarad ($p < 0.01$, $n = 12$; Fig. 1*F*). Further effects mediated by U-II including the voltage dependences of activation and inactivation were examined. We observed a significant shift of the steady-state inactivation potentials of $I_{Ca,L}$ by 8.5 mV in the depolarized direction (V_{half} from −32.6 ± 0.6 to −24.1 ± 0.8 mV, $n = 11$; Fig. 1, *G* and *I*), whereas the activation potential did not change significantly (V_{half} from −12.6 ± 0.5 to −12.8 ± 0.8 mV, $n = 9$; Fig. 1, *H* and *I*). These results suggest that the increase in $I_{Ca,L}$ observed after the application of U-II may be due to the retention of a decreased proportion of inactivated channels.

U-IIR Mediates U-II-induced Increase in $I_{Ca,L}$—U-IIR is the functional receptor for U-II *in vivo* (2). We examined U-IIR participation in $I_{Ca,L}$ responses to U-II by examining the expression profile in rat ventricular myocytes. RT-PCR analysis demonstrated that the transcripts for U-IIR (predicted size of amplicon is 537 bp) were present in adult rat ventricular myocytes. Negative control reactions in which reverse transcriptase was excluded from the RT step did not yield any PCR products

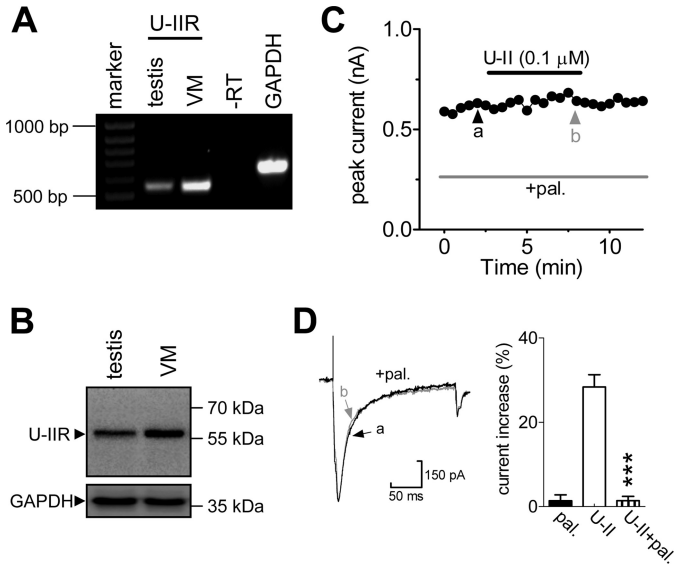

FIGURE 2. **U-II increases $I_{Ca,L}$ via the activation of U-IIR.** *A*, detection of U-IIR mRNA in adult rat ventricular myocytes. Total RNA from rat testis was used as a positive control. *−RT*, negative control, RT-PCR without the addition of enzyme. *B*, Western blot analysis showed the expression of U-IIR protein in rat ventricular myocytes. GAPDH was used as a loading control. The blots shown are representative of three experiments. *C* and *D*, time course (*C*) and summary of results (*D*) showing that treatment of ventricular myocytes with palosuran (*pal.*) (1 μM for 30 min) completely abolished the increase in $I_{Ca,L}$ induced by 0.1 μM U-II ($n = 9$). Application of palosuran (1 μM) alone had no significant effect on $I_{Ca,L}$ ($n = 7$). *Letters* (*a* and *b*) indicate the points used for sample traces. ***, $p < 0.001$ *versus* 0.1 μM U-II. *Error bars* represent S.E. *VM*, ventricular myocytes.

(Fig. 2*A*). Protein levels of U-IIR were assessed by immunoblotting with subunit-specific antibodies. Immunoblotting analysis revealed that U-IIR is endogenously expressed in adult rat ventricular myocytes. The rat testis expresses U-IIR and was therefore used as a positive control (Fig. 2*B*). We next determined the involvement of U-IIR in U-II-induced changes in $I_{Ca,L}$. Palosuran (1 μM), a specific U-IIR antagonist, alone had no significant effect on $I_{Ca,L}$ in adult rat ventricular myocytes (increase of 1.5 ± 1.2%, $n = 7$), whereas pretreatment of cells with palosuran (1 μM) completely abolished the U-II-induced $I_{Ca,L}$ response (increase of 2.6 ± 1.3%, $n = 9$, $p < 0.001$; Fig. 2, *C* and *D*), suggesting that the U-II-induced increase in $I_{Ca,L}$ was dependent on U-IIR.

U-II-induced Changes in $I_{Ca,L}$ Require the βγ Subunits of $G_{i/o}$—U-IIR is a G-protein-coupled receptor and has been shown to couple to $G_{q/11}$ in the cardiomyocytes (2, 32). To investigate the potential involvement of heterotrimeric G-proteins, cells were dialyzed with the non-hydrolyzable GDP analog GDP-β-S (1 mM). GDP-β-S completely abolished the increase in $I_{Ca,L}$ induced by U-II (increase of 2.7 ± 1.1%, $n = 8$; Fig. 3*A*), indicating the requirement for G-protein activation. We next determined the involvement of $G_{q/11}$ in the response mediated by U-IIR. Because of a lack of commercially available specific $G_{q/11}$ inhibitors, an adenovirus-based shRNA knockdown approach was used to examine the effect of U-II on $I_{Ca,L}$ in G_q-silenced ventricular myocytes. Western blot analysis showed that the expression of G_q was significantly reduced in cells transduced with G_q shRNA (Ad-G_q-shRNA) compared with the cells transduced with control shRNA (Ad-NC-shRNA; Fig. 3*B*). Knockdown of G_q did not affect the U-II-induced $I_{Ca,L}$ increase (increase of 27.9 ± 1.7%, $n = 12$; Fig. 3*C*), and there was no significant difference in the $I_{Ca,L}$ density between control shRNA and non-transduced control cells (Figs. 1*F* and 3*C*). These results support the hypothesis that the U-II-induced increase in $I_{Ca,L}$ is independent of $G_{q/11}$ in adult rat ventricular myocytes. In cultured ventricular myocytes (48 h), the current density of $I_{Ca,L}$ slightly, but not significantly, decreased at 0 mV (6.6 ± 0.4 pA/picofarad for control, $n = 9$; 5.9 ± 1.1 pA/picofarad for cultured cells, $n = 11$; Fig. 3*D*). In addition, the voltage dependence of $I_{Ca,L}$ activation and inactivation was also measured in control and in cultured cells. Similar values for half-maximal activation and inactivation voltage (V_{half}) (V_{half} from −13.1 ± 0.4 to −12.3 ± 0.6 mV for activation curve, $n = 9$; V_{half} from −29.7 ± 0.7 to −28.6 ± 0.9 mV for inactivation curve, $n = 12$; Fig. 3*E*) and slope factor (k) (k from 7.7 ± 0.6 to 7.5 ± 0.9 mV for activation curve, $n = 9$; k from 8.9 ± 0.6 to 9.1 ± 0.8 mV for inactivation curve, $n = 12$; Fig. 3*E*) were obtained in both groups. We next examined the involvement of different G-protein subtypes in the U-II-mediated modulation of $I_{Ca,L}$. Inactivation of G_s by pretreating ventricular myocytes with cholera toxin (0.5 μg/ml for 24 h) did not affect the ability of U-II to increase $I_{Ca,L}$ (increase of 32.2 ± 3.1%, $n = 10$; Fig. 3*F*). Conversely, inhibition of $G_{i/o}$ by pretreating ventricular myocytes with PTX (0.2 μg/ml for 24 h) abolished the stimulatory effect of U-II (increase of 1.3 ± 2.1%, $n = 9$; Fig. 3*F*). These results indicate that $G_{i/o}$ is involved in the transduction pathways leading to the increase in $I_{Ca,L}$ in response to U-IIR stimulation.

The potential role of the native βγ subunits (Gβγ) of $G_{i/o}$-protein in the U-IIR-mediated increase of $I_{Ca,L}$ was examined further. Intracellular infusion of synthetic peptide QEHA was used to bind Gβγ subunits released after receptor activation, thus preventing the activation of the upstream effectors. Application of QEHA (10 μM) through the recording pipette blocked the U-II-induced response (increase of 2.8 ± 3.2%, $n = 9$; Fig. 3, *G* and *H*), whereas similar dialysis of a scrambled peptide, SKEE (10 μM), did not alter the ability of U-II to increase $I_{Ca,L}$ (increase of 27.5 ± 1.5%, $n = 10$; Fig. 3*H*). Together, these findings suggest that the Gβγ subunit of the $G_{i/o}$-protein complex mediates the U-II-induced increase in $I_{Ca,L}$.

U-IIR-mediated Stimulation of $I_{Ca,L}$ Involves the Class I PI3K but Not Akt—Next, we investigated in detail the mechanism underlying the U-IIR-mediated $I_{Ca,L}$ increase. Examination of the potential involvement of intracellular signaling pathways revealed no evidence for the involvement of PKA. Preincubation of cells with the PKA inhibitor KT-5720 (1 μM) did not alter the ability of U-II to increase $I_{Ca,L}$ (increase of 27.6 ± 1.8%, $n = 10$; Fig. 4, *A* and *C*). Similar results were obtained following addition of another PKA inhibitor, protein kinase inhibitor 5–24 (increase of 28.2 ± 2.1%, $n = 9$; Fig. 4, *B* and *C*). Pretreatment of ventricular myocytes with 1 μM KT-5720 abolished the ability of forskolin (20 μM) to increase PKA activity (Fig. 4*D*), thus confirming the inhibitory effect of KT-5720. Previous studies have shown that the immediate downstream mediator of Gβγ is PI3K; therefore, to examine the role of PI3K in the response mediated by U-II, we first determined PI3K activity in ventricular myocytes. U-II significantly induced phosphatidylinositol 3,4,5-trisphosphate accumulation, and this effect was blocked by pretreatment of the cells with the PI3K inhibitor

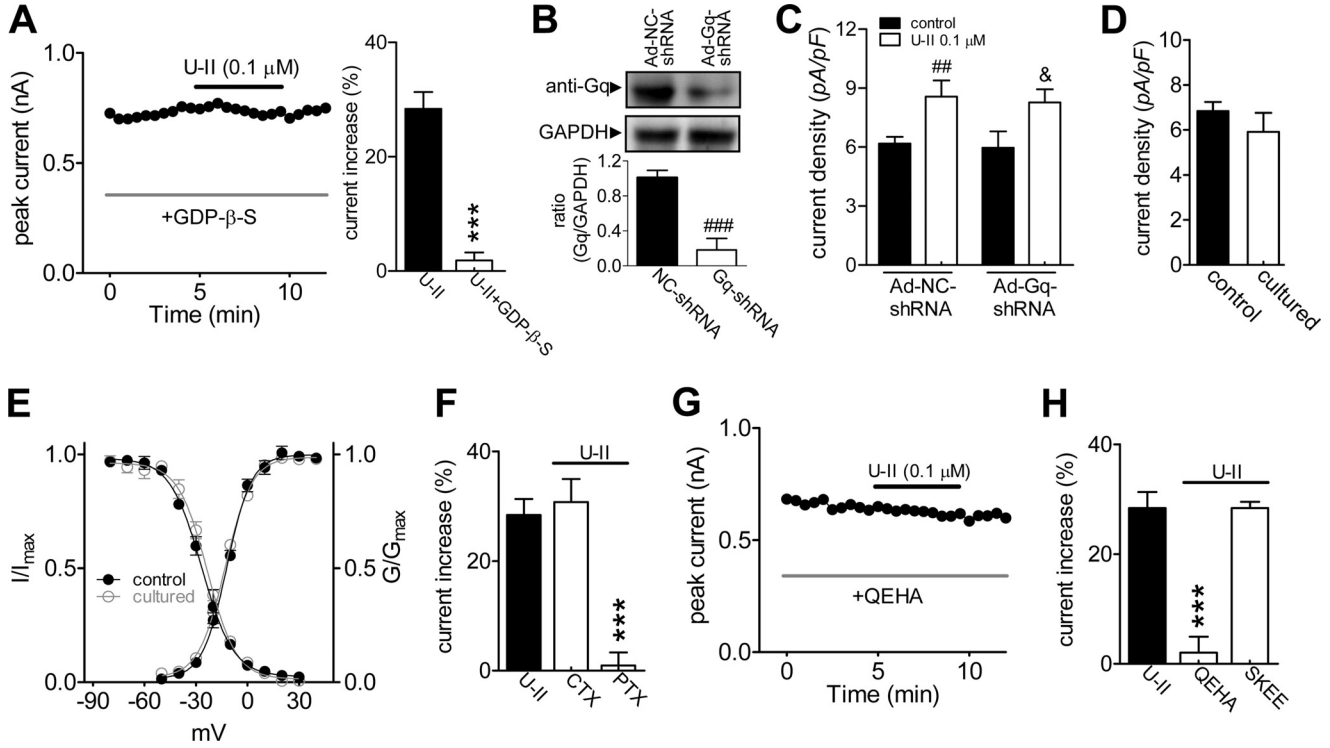

FIGURE 3. **The $\beta\gamma$ subunits of $G_{i/o}$-protein are involved in the U-II-induced response.** *A*, time course (*left panel*) and summary of results (*right panel*) showing the effect of U-II (0.1 μM) on $I_{Ca,L}$ in the presence of GDP-β-S (1 mM applied intracellularly) ($n = 8$). *B*, protein expression of G_q measured by Western blotting in control shRNA (Ad-NC-shRNA)- and G_q shRNA-treated (Ad-G_q-shRNA) groups. GAPDH was used as a loading control. The blots shown are representative of three individual experiments. *C*, summary of results showing the effect of G_q shRNA on 0.1 μM U-II-induced $I_{Ca,L}$ increase. $I_{Ca,L}$ were recorded from ventricular myocytes transfected with control shRNA ($n = 10$) or G_q shRNA ($n = 12$). *D*, summary of results showing the current density of $I_{Ca,L}$ at 0 mV in control cells ($n = 9$) compared with the ventricular myocytes cultured for 48 h ($n = 11$). *E*, similar values for half-maximal activation ($n = 9$) and inactivation ($n = 12$) voltage (V_{half}) and slope factor (k) were obtained in both control cells and the ventricular myocytes cultured for 48 h. *F*, summary of results showing the effect of 0.1 μM U-II on $I_{Ca,L}$ following cholera toxin (*CTX*; 0.5 μg/ml pretreated for 24 h; $n = 10$) or PTX pretreatment (0.2 μg/ml pretreated for 24 h; $n = 9$). *G*, time courses showing the effects of 0.1 μM U-II on $I_{Ca,L}$ in the presence of QEHA (intracellular application). *H*, summary of results showing the effects of 0.1 μM U-II on $I_{Ca,L}$ in the presence of QEHA ($n = 9$) or SKEE (intracellular application; $n = 10$). ***, $p < 0.001$ *versus* 0.1 μM U-II; ##, $p < 0.01$ *versus* Ad-NC-shRNA; ###, $p < 0.001$ *versus* Ad-NC-shRNA; &, $p < 0.05$ *versus* Ad-G_q-shRNA. *Error bars* represent S.E. *pF*, picofarad.

wortmannin (0.5 μM) (Fig. 4*E*). Furthermore, wortmannin pretreatment completely abolished the increase of $I_{Ca,L}$ induced by U-II (increase of 0.9 ± 2.5%, $n = 9$; Fig. 4, *F* and *H*). It should be noted that pretreatment of cells with CH5132799 (1 μM), which selectively inhibits class I PI3Ks, also blocked the U-II-induced $I_{Ca,L}$ response (increase of 2.3 ± 1.1%, $n = 9$; Fig. 4*H*). Akt is a common downstream target of PI3K (33–35). Therefore, we examined whether U-II action is mediated by Akt activation. We assayed the activity of Akt in ventricular myocytes treated with 0.1 μM U-II. Fig. 4*I* illustrates that the level of phosphorylated Akt increased following treatment with U-II (0.1 μM), whereas total Akt did not change. This effect was abolished by Akt inhibitor III (10 μM; Fig. 4*I*). To further explore the role of Akt in the modulation of $I_{Ca,L}$ by U-II, cells were pretreated with Akt inhibitor III prior to 0.1 μM U-II stimulation. Interestingly, in the presence of Akt inhibitor III (10 μM), U-II still caused a significant increase in $I_{Ca,L}$ (increase of 27.7 ± 4.1%, $n = 11$; Fig. 4, *G* and *H*). Taken together, these results suggest that U-II increases $I_{Ca,L}$ through PI3K activation (likely via the class I PI3K) but independently of PKA or Akt signaling.

U-IIR-induced Stimulation of $I_{Ca,L}$ Involves PKC—PKC activation has been shown to modulate L-type Ca^{2+} channels (22, 36) and can act as a downstream effector of G$\beta\gamma$ activation (37). We further investigated the role of PKC in U-II-induced changes in $I_{Ca,L}$. U-II (0.1 μM) significantly increased PKC activity (~2.3-fold) in rat ventricular myocytes (Fig. 5*A*). This response was abolished in cells pretreated with the class I PI3K inhibitor CH5132799 (1 μM) (Fig. 5*A*). Calphostin C (50 nM), an inhibitor of both novel and classic PKC isoforms, abolished the ability of U-II to increase $I_{Ca,L}$ (increase of 1.5 ± 1.6%, $n = 10$; Fig. 5*B*). Similar results were obtained with another classic and novel PKC antagonist, chelerythrine chloride (1 μM) (increase of 1.3 ± 2.9%, $n = 9$; Fig. 5*B*). Interestingly, the inhibition of PKC on U-II-induced responses by these antagonists was reproduced by Ro 31-8220 (2 μM), which blocks only classic PKC isoforms (increase of 1.9 ± 1.8%, $n = 10$; Fig. 5*B*). Application of calphostin C (50 nM), chelerythrine chloride (1 μM), or Ro 31-8220 (2 μM) alone had no significant effect on $I_{Ca,L}$ in adult rat ventricular myocytes (increase of −1.7 ± 1.9% for calphostin C, $n = 6$; increase of 2.1 ± 2.3% for chelerythrine, $n = 5$; increase of −1.0 ± 2.1% for Ro 31-8220, $n = 6$; Fig. 5*B*). In contrast to novel PKC isoforms, activation of classic PKC isoforms requires cytoplasmic Ca^{2+}. Intracellular dialysis of the fast Ca^{2+} chelator BAPTA (20 mM), but not the inactive analog dn-BAPTA, completely abolished the U-II-mediated response (increase of 1.3 ± 2.1% for BAPTA, $n = 10$; increase of 27.5 ± 3.6% for dn-BAPTA, $n = 8$; Fig. 5, *C* and *D*), thus supporting the involvement of classic PKC isoforms in this process.

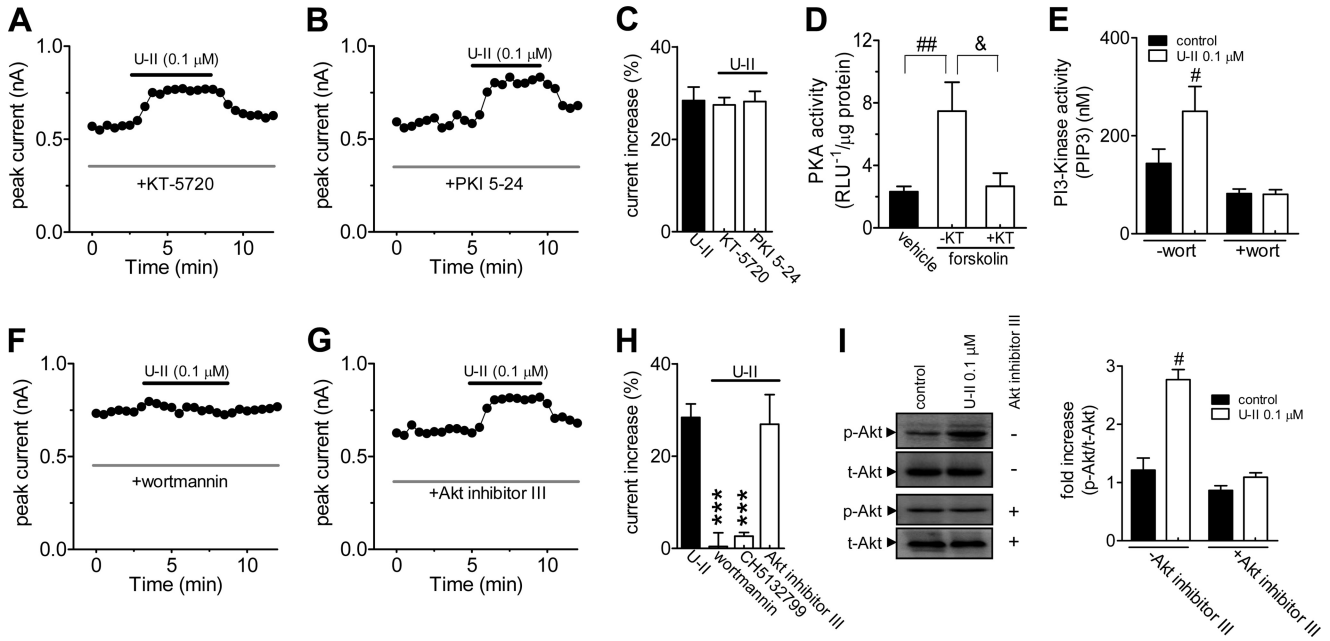

FIGURE 4. **U-IIR-mediated $I_{Ca,L}$ increase requires PI3K.** *A* and *B*, time course of changes in $I_{Ca,L}$ amplitude mediated by 0.1 μM U-II in the presence of either KT-5720 (1 μM for 30 min; *A*) or protein kinase inhibitor (*PKI*) 5–24 (1 μM intracellular application; *B*). *C*, summary of results showing the effects of U-II on $I_{Ca,L}$ in the presence of either KT-5720 ($n = 10$) or protein kinase inhibitor 5–24 ($n = 9$) as indicated in *A* and *B*. *D*, bar graph showing the activity of PKA in control cells, in ventricular myocytes treated with 20 μM forskolin, and in ventricular myocytes preincubated with KT-5720 (*KT*) (1 μM for 30 min) and then treated with 20 μM forskolin. *E*, U-II (0.1 μM) induced a significant increase in PI3K activity in the ventricular myocytes. This was blocked by the pretreatment of cells with wortmannin (*wort*) (0.5 μM for 30 min). All experiments were performed in triplicate with similar results. *F* and *G*, time course showing the stimulatory effects of 0.1 μM U-II on $I_{Ca,L}$ in the presence of wortmannin (0.5 μM for 30 min; *F*) and CH5132799 (1 μM for 30 min; *G*). *H*, summary of results showing that treatment of ventricular myocytes with either wortmannin ($n = 9$) or CH5132799 ($n = 9$), but not Akt inhibitor III (10 μM, $n = 11$), completely abolished the 0.1 μM U-II-induced $I_{Ca,L}$ increase. *I*, pretreatment of cells with Akt inhibitor III (10 μM) abolished 0.1 μM U-II-induced Akt phosphorylation. The blots shown are representative of three experiments. ***, $p < 0.001$ *versus* 0.1 μM U-II; #, $p < 0.05$ *versus* vehicle; ##, $p < 0.01$ *versus* vehicle; &, $p < 0.05$ *versus* 20 μM forskolin. *Error bars* represent S.E. *RLU*, relative light units; *p-Akt*, phosphorylated Akt; *t-Akt*, total Akt; *PIP3*, phosphatidylinositol 3,4,5-trisphosphate.

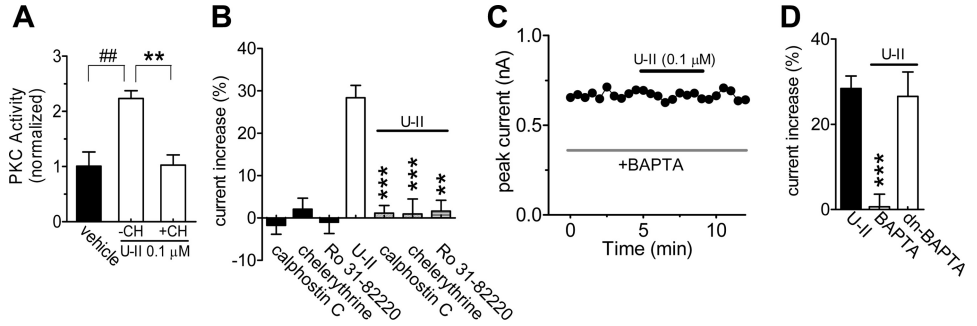

FIGURE 5. **U-II increases $I_{Ca,L}$ through activation of PKC.** *A*, bar graph showing the activity of PKC in control cells, in ventricular myocytes treated with 0.1 μM U-II, and in ventricular myocytes pre-incubated with CH5132799 (*CH*) (1 μM for 30 min) and then treated with 0.1 μM U-II. *B*, summary of results showing the effect of 0.1 μM U-II on $I_{Ca,L}$ in the presence of calphostin C (50 nM for 30 min; $n = 10$), chelerythrine chloride (1 μM for 30 min; $n = 9$), and Ro 31-8220 (2 μM for 30 min; $n = 10$). Application of calphostin C (50 nM; $n = 6$), chelerythrine chloride (1 μM; $n = 5$), or Ro 31-8220 (2 μM; $n = 6$) alone had no significant effect on $I_{Ca,L}$. *C* and *D*, time course and summary of results showing the effect of U-II (0.1 μM) on the $I_{Ca,L}$ amplitude in the presence of BAPTA (20 mM intracellular application; $n = 10$) or dn-BAPTA (intracellular application; $n = 8$). **, $p < 0.01$ *versus* 0.1 μM U-II; ***, $p < 0.001$ *versus* 0.1 μM U-II; ##, $p < 0.01$ *versus* vehicle. *Error bars* represent S.E.

The Classic PKCβ1 Isoform Is Involved in U-II Response—Next, we aimed to determine the exact PKC isoform involved in the U-II-induced $I_{Ca,L}$ increase. To achieve this, we first investigated the protein expression profiles of classic PKC isoforms in rat ventricular myocytes. Western blot analysis revealed that PKCα, PKCβ_1, and PKCβ_2 are expressed in adult rat ventricular myocytes, whereas PKCγ could not be detected (Fig. 6*A*). Rat brain expresses all four classic PKC isoforms and was used as a positive control for the various PKC isoform antisera (Fig. 6*A*). Pretreatment of cells with HBDDE (1 μM), a PKCα and PKCγ inhibitor, did not affect the stimulatory effects of U-II on $I_{Ca,L}$ (increase of 26.9 ± 3.3%, $n = 10$; Fig. 6, *B* and *D*). In contrast, pretreating ventricular myocytes with the PKCβ antagonist LY333531 (0.2 μM) abolished the U-II-mediated change in $I_{Ca,L}$ (increase of 1.8 ± 2.1%, $n = 9$; Fig. 6, *C* and *D*). In addition, dialysis of cells with βIV5-3 (0.1 μM), a PKCβ_1-specific inhibitor, completely blocked the U-II-induced $I_{Ca,L}$ increase (increase of 0.9 ± 1.2%, $n = 9$; Fig. 6*E*). Application of scrambled βIV5-3 (0.1 μM) (increase of 28.1 ± 1.9%, $n = 9$; Fig. 6*E*) or the PKCβ_2-specific inhibitor βIIV5-3 (0.1 μM) (increase of 27.3 ± 3.1%, $n = 10$; Fig. 6*E*) did not elicit this effect. Together, these results suggest that PKCβ_1 may be involved in the U-II-induced increase in $I_{Ca,L}$. To confirm this, we used an adenovirus-based shRNA approach to knock down PKCβ_1 in

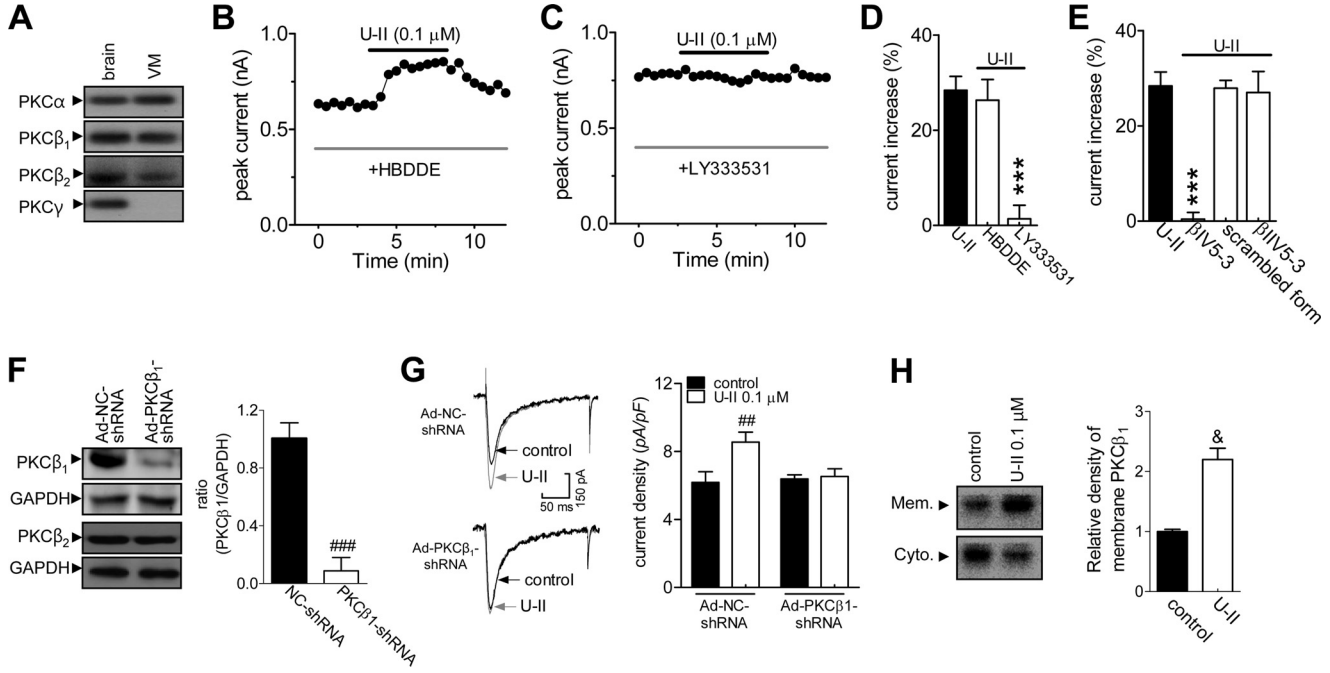

FIGURE 6. **U-II increases $I_{Ca,L}$ via activation of the classic PKCβ_1 pathway.** *A*, Western blots were incubated with rabbit polyclonal antibodies (PKCα, PKCβ_2, and PKCγ) or mouse monoclonal antibodies (PKCβ_1) to determine the protein levels of classic PKC isoforms in rat ventricular myocytes. Rat brain proteins were used as positive controls. The blots shown are representative of three experiments. *B* and *C*, time courses of the effect of U-II (0.1 μM) on $I_{Ca,L}$ in the presence of HBDDE (1 μM; *B*) and LY333531 (0.2 μM; *C*). *D* and *E*, summary of results showing the effect of U-II (0.1 μM) on $I_{Ca,L}$ in the presence of HBDDE (1 μM for 30 min; $n = 10$; *D*), LY333531 (0.2 μM for 30 min; $n = 9$; *D*), βIV5-3 (0.1 μM intracellular application; $n = 9$; *E*), scrambled βIV5-3 (0.1 μM intracellular application; $n = 9$, *E*), and βIIV5-3 (0.1 μM intracellular application; $n = 10$; *E*). *F*, protein expression of PKCβ_1 and PKCβ_2 was measured by Western blotting in control shRNA (Ad-NC-shRNA) and PKCβ_1 shRNA-treated (Ad-PKCβ_1-shRNA) groups. The blots shown are representative of three experiments. GAPDH was used as a loading control. *G*, representative current traces and summary of results showing the effect of PKCβ_1 shRNA on 0.1 μM U-II-induced $I_{Ca,L}$ increase in rat ventricular myocytes ($n = 9$). *H*, effect of U-II on membrane PKCβ_1 expression. Cells were treated with vehicle or U-II (0.1 μM) for 15 min. The blots shown are representative of three independent experiments. ***, $p < 0.001$ *versus* 0.1 μM U-II; ##, $p < 0.01$ *versus* Ad-NC-shRNA; ###, $p < 0.001$ *versus* Ad-NC-shRNA; &, $p < 0.05$ *versus* control. *Error bars* represent S.E. *Cyto.*, cytosolic fraction; *Mem.*, membrane fraction.

ventricular myocytes. Western blot analysis revealed that the expression of PKCβ_1 was substantially reduced in cells transduced with PKCβ_1-specific shRNA (Ad-PKCβ_1-shRNA) compared with the cells transduced with control shRNA (Ad-NC-shRNA) (Fig. 6*F*), whereas the expression of PKCβ_2 was not affected. Knockdown of PKCβ_1 in ventricular myocytes almost completely eliminated the U-II-mediated increase in $I_{Ca,L}$ (increase of 1.3 ± 0.7%, $n = 9$; Fig. 6*G*). Cellular activation of PKC is linked to its translocation and binding to the plasma membrane. Therefore, to support the results from the previous experiments, we examined the translocation of PKCβ_1 from the cytosolic to the membrane fractions of the cell following treatment with U-II. Western blot analysis indicated an increase of membrane-bound PKCβ_1 and a decrease in the cytosolic fraction following stimulation with U-II (0.1 μM; Fig. 6*H*). Collectively, these results suggest that the U-II-mediated increase in $I_{Ca,L}$ occurs through the classic PKCβ_1 pathway.

U-II Increased the Amplitude of Sarcomere Shortening—L-type Ca^{2+} channels are at the top of a cascade of events that initiate excitation-contraction coupling and thus regulate the strength of cardiac contraction (18–20). L-type Ca^{2+} channel blockers can cause a negative inotropism; conversely, any agent that increases $I_{Ca,L}$ might, in theory, serve as a positive inotrope (20). To further examine the functional implications of the $I_{Ca,L}$ increase induced by U-II, we tested the effects of U-II on cardiomyocyte contractility in rat ventricular myocytes. Our results showed that application of U-II (0.1 μM) resulted in a rapid (usually within 5 min after administration) increase in the amplitude of sarcomere shortening (increase of 30.8 ± 3.1%, $n = 12$ from five hearts; Fig. 7, *A* and *B*). The effects of U-II on cardiomyocyte shortening in response to depolarizing pulses were reversible after washout of U-II from the bath solution (Fig. 7*B*). We next determined the involvement of U-IIR in U-II-induced changes in cardiomyocyte shortening. Our results showed that pretreatment of cells with palosuran (1 μM), a specific U-IIR antagonist, abolished the U-II-induced response (increase of 2.1 ± 1.7%, $n = 6$ from three hearts; Fig. 7*C*), suggesting the involvement of U-IIR in the U-II-induced increase in the amplitude of sarcomere shortening. Furthermore, pretreating ventricular myocytes with the PKCβ antagonist LY333531 (0.2 μM) completely abolished the U-II-mediated change in sarcomere shortening (increase of 3.5 ± 2.8%, $n = 6$ from three hearts; Fig. 7*C*), whereas the PKCα inhibitor HBDDE (1 μM) elicited no such effect (increase of 27.6 ± 1.9%, $n = 10$ from six hearts; Fig. 7*C*). To further verify that this U-II-induced response was mediated by the $I_{Ca,L}$ increase, we investigated whether Bay K8644, an L-type Ca^{2+} channel agonist, would occlude the U-IIR-mediated increase in the amplitude of sarcomere shortening. Indeed, Bay K8644 at 0.5 μM induced a significant increase in $I_{Ca,L}$ (increase of 37.6 ± 3.1%, $n = 7$; Fig. 7*D*). Application of Bay K8644 (0.5 μM) to ventricular myocytes mimicked the U-II-induced increase in the amplitude of sarcomere shortening (Fig. 7, *E* and *F*). Notably, application of U-II (0.1 μM) after the maximum Bay K8644-induced

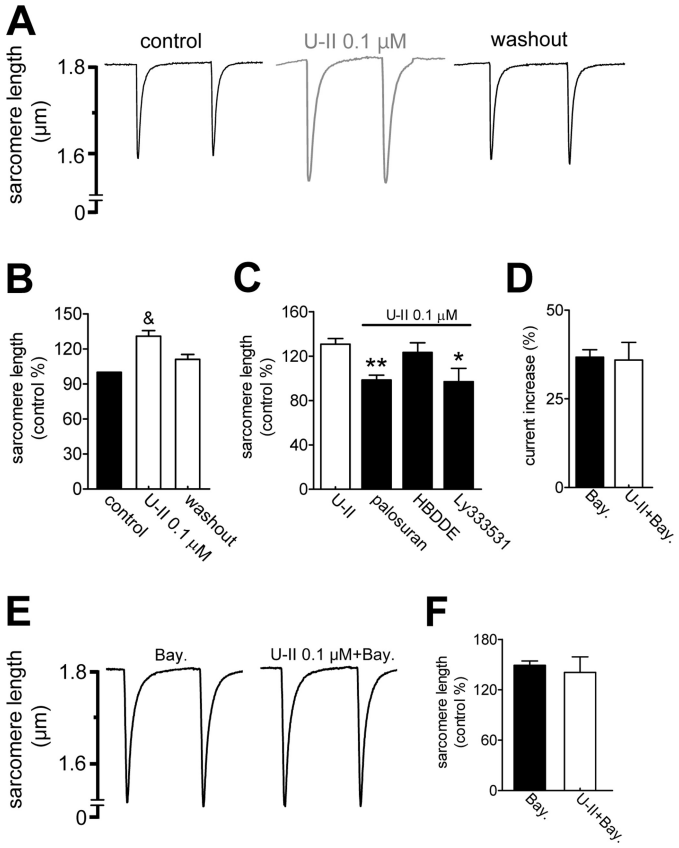

FIGURE 7. **U-II increases the amplitude of sarcomere shortening.** *A* and *B*, representative recordings (*A*) and summary data (*B*) of sarcomere shortening of ventricular myocytes under control conditions, exposure to 0.1 μM U-II for 5 min, and washout ($n = 12$). The *vertical axis* shows absolute sarcomere length in micrometers. *C*, effect of U-II (0.1 μM) on cardiomyocyte contractility in the presence of palosuran (1 μM for 30 min; $n = 6$), HBDDE (1 μM for 30 min; $n = 10$), and LY333531 (0.2 μM for 30 min; $n = 6$). *D*, summary of results showing the effect of U-II (0.1 μM) on $I_{Ca,L}$ in the presence of Bay K8644 (*Bay.*) (0.5 μM for 30 min; $n = 7$). *E* and *F*, representative recordings (*E*) and summary data (*F*) showing the effect of U-II (0.1 μM) on sarcomere shortening in the presence of Bay K8644 (0.5 μM; $n = 11$). *, $p < 0.05$ *versus* U-II at 0.1 μM; **, $p < 0.01$ *versus* U-II at 0.1 μM; &, $p < 0.05$ *versus* control. *Error bars* represent S.E.

response failed to produce any further increase either in $I_{Ca,L}$ (increase of 35.9 ± 6.5%, $n = 7$; Fig. 7*D*) or in the amplitude of sarcomere shortening (Fig. 7, *E* and *F*). These results together suggest that U-II increased the amplitude of sarcomere shortening through a U-IIR-dependent PKCβ and L-type Ca^{2+} channel pathway.

DISCUSSION

The present study provides mechanistic data describing a novel functional role of U-II in modulating L-type Ca^{2+} channels as well as sarcomere shortening in adult rat ventricular myocytes. These results suggest that this response is mediated by U-IIR coupled to the $\beta\gamma$ subunits of $G_{i/o}$-proteins and subsequent activation of the class I PI3K-dependent PKCβ_1 isoform. A schematic diagram of this proposed pathway is shown in Fig. 8.

U-IIR activation is detected through PTX-insensitive G-protein $G_{q/11}$ coupling sequentially to phospholipase C (2, 32). Interestingly, in adult rat ventricular myocytes, we found that the $\beta\gamma$ subunits of PTX-sensitive $G_{i/o}$-protein are involved in the U-IIR-mediated L-type Ca^{2+} channel stimulation because 1) the effect was blocked by the nonselective G-protein inhibitor GDP-β-S and 2) pretreatment with PTX, but not cholera toxin, abolished the response to U-II, indicating the involvement of $G_{i/o}$ in rat ventricular myocytes. It has been suggested previously that $G_{i/o}$ can interact directly with L-type Ca^{2+} channels (38); however, such a mechanism is unlikely to be involved in our system. We did find the involvement of G$\beta\gamma$ subunits in the U-II-induced response because pipette application of the peptide QEHA, which disrupts interactions between G$\beta\gamma$ subunits and Ca^{2+} channels, but not its scrambled peptide SKEE abolished U-II-induced stimulation. However, G$\beta\gamma$ did not seem to interact with the L-type Ca^{2+} channels because the U-II-induced response was further blocked by the inhibition of downstream protein kinases. Importantly, the outcome of G$\beta\gamma$ regulation of Cav1.2 was a reduction in $I_{Ca,L}$ due to direct interaction with the N terminus of α1C subunits (39). The apparent independence of G$\beta\gamma$ subunits in the modulation of L-type calcium channels may indicate that rat ventricular myocytes express a Ca^{2+} channel that is insensitive to the G$\beta\gamma$ subunits of $G_{i/o}$. An alternative hypothesis is that different Cav1.2 channel splice variants are able to generate different L-type Ca^{2+} channel functions (40). For example, alternative splicing of the Cav1.2 channel changes the sensitivity of the L-type Ca^{2+} channel to dihydropyridines (41). In addition, it is possible that U-IIR-mediated G$\beta\gamma$ activation does not result in a functional increase in L-type Ca^{2+} channel current in adult rat ventricular myocytes.

Presently, it is unclear how G$\beta\gamma$ stimulates L-type Ca^{2+} channel activity. G$\beta\gamma$ subunits can activate PKA to modulate various targets including calcium channels (42, 43). For example, $I_{Ca,L}$ recorded from isolated cardiomyocytes were shown to be increased by β-adrenergic receptors via the cAMP/PKA-dependent pathway (44). In contrast, $I_{Ca,L}$ inhibition by CB1 cannabinoid receptor activation was prevented by the application of PKA inhibitors (45). Similarly, Cav1.2 current inhibition by integrin receptor activation was blocked by the addition of the PKA inhibitor H89 (46). However, in the present study, we found that the stimulatory effect of U-II on $I_{Ca,L}$ was PKA-independent, which suggests that other non-cAMP/PKA-dependent mechanisms are involved in the stimulatory effect of U-II. PI3K (particularly PI3Kγ) is a known downstream target of G$\beta\gamma$ signaling, and there is evidence that G$\beta\gamma$ stimulates Cav1.2 via PI3K (47). In this study, we found that the response to U-II was abolished by the selective PI3K inhibitors, suggesting that PI3K also participates in the U-IIR/G$\beta\gamma$ pathway in rat ventricular myocytes. In contrast, the stimulatory effect of U-II on PKC activity was abolished by PI3K blockade, suggesting that PKC is downstream of PI3K rather than the reverse.

Next, we wished to determine how PI3K activates PKC. Phosphatidylinositol 3,4,5-trisphosphate, the lipid product of PI3K, targets several different second messengers (48, 49) including PKC. Furthermore, PI3Kγ itself has serine kinase activity, and this could lead to PKC activation (50–53). The G$\beta\gamma$/PI3K pathway has been reported to regulate chloride channels in oocytes and has been linked to phosphatidylinositol 3,4,5-trisphosphate-dependent activation of PKCζ, an atypical PKC that is insensitive to both Ca^{2+} and diacylglycerol (54, 55). In addition, the G$\beta\gamma$/PI3K pathway has been shown to activate

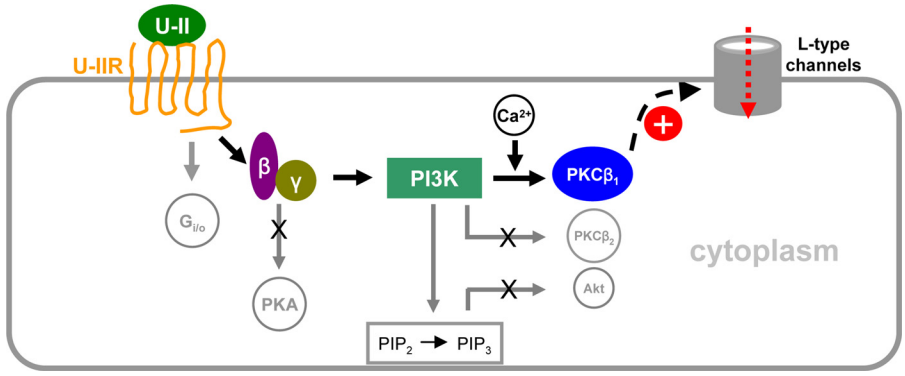

FIGURE 8. **Proposed signaling pathway involved in the effect of U-II on L-type Ca^{2+} channels.** U-II binds to U-IIR, which is coupled to the G-protein $G_{i/o}$, causing it to release the $G\beta\gamma$ subunits. Activation of PI3K by the $G\beta\gamma$ subunit causes an increase in PKCβ_1 activity and subsequent stimulation of the L-type Ca^{2+} channels. PI3K catalyzes the conversion of phosphatidylinositol 4,5-bisphosphate (*PIP_2*) to phosphatidylinositol 3,4,5-trisphosphate (*PIP_3*), which serves as a second messenger that helps to activate Akt. Neither PKA, Akt, PKCβ_2, nor direct interaction between $G\beta\gamma$ and L-type Ca^{2+} channel is necessary for the U-IIR-mediated increase of $I_{Ca,L}$. Whether PKCβ_1 directly phosphorylates L-type Ca^{2+} channels or acts on an intermediate protein remains unclear.

a novel PKC isoform in rabbit portal vein myocytes (50). Conversely, the U-IIR-induced response is blocked with calphostin C. Calphostin C inhibits both classic and novel PKCs but not atypical PKCs. Furthermore, the effects of U-II in the present study were also inhibited when selective antagonists of classic PKCs and a fast intracellular calcium chelator were used, leading us to the conclusion that classic PKC isoforms are involved.

The following data suggest that PKCβ_1 is involved in the U-II-induced increase in $I_{Ca,L}$. 1) Pharmacological inhibition of PKC$_\beta$, but not PKCα, completely abolished the increase of U-II on $I_{Ca,L}$. 2) PKCβ_1 has been identified in rat ventricular myocytes, and U-II increases the membrane expression of PKCβ_1. 3) Pharmacological inhibition of PKCβ_1 or knockdown with shRNA blocked the U-II-induced $I_{Ca,L}$ response. These results are supported by previous studies showing that PKC activation increases $I_{Ca,L}$ in neonatal mouse ventricular myocytes (56). It has also been shown that PKC phosphorylates the Cav1.2 α1C calcium channel subunit, resulting in the up-regulation of L-type Ca^{2+} channel activity (57). Similar results have been reported in rat portal vein myocytes (50). In contrast, a PKC-induced $I_{Ca,L}$ decrease has been described in the heart (58, 59) and cerebral artery smooth muscle cells (60). Biphasic effects of PKC and no effect of PKC activation on L-type Ca^{2+} channels have also been reported (61, 62). Although the regulation of L-type Ca^{2+} channels by PKC remains controversial, the differential modulation of L-type Ca^{2+} channel activity by PKC may also involve different parameters. First, the expression and/or activation of endogenous PKC isoforms is tissue/cell-specific, and remarkable heterogeneity across PKC-dependent signal transduction pathways exists including that for ion channel modulation (63, 64). As described in the present study, we suggest that the PKCβ_1 isoform is involved in the U-II-induced $I_{Ca,L}$ response. Second, PKC modulation of L-type Ca^{2+} channels may involve PKC-interacting proteins; this is the case for the Cav2.2 N-type channel (65). PKC-interacting proteins confer specificity on individual PKC isoforms by regulating their activity and cellular location, endowing isoforms with the ability to mediate specific cellular functions (66, 67). Finally, cell-specific splice variants of Cav1.2 α1C (68) or β subunits (69) might modulate the pharmacological properties of L-type Ca^{2+} channels in different ways. Therefore, we cannot exclude the possibility that an intermediate protein, phosphorylated by a different PKC isoform, may be involved in the observed U-IIR-mediated response.

In conclusion, the present study provides evidence of new mechanisms involved in the modulation of L-type Ca^{2+} channels by U-II in adult rat ventricular myocytes. We propose that the marked increase in $I_{Ca,L}$ induced by U-II is mediated through U-IIR and involves the $G\beta\gamma$ subunits of $G_{i/o}$ and downstream class I PI3K-dependent activation of the PKCβ_1 pathway. We found no evidence of a role for PKA and Akt signaling. This novel mechanism may contribute to the physiological functions of U-II including ventricular contraction in the mammalian cardiovascular system.

Acknowledgments—We thank Drs. Xiaofei Zhou and Kun Chen for technical assistance and invaluable comments.

REFERENCES

1. Pearson, D., Shively, J. E., Clark, B. R., Geschwind, I. I., Barkley, M., Nishioka, R. S., and Bern, H. A. (1980) Urotensin II: a somatostatin-like peptide in the caudal neurosecretory system of fishes. *Proc. Natl. Acad. Sci. U.S.A.* **77,** 5021–5024
2. Vaudry, H., Do Rego, J. C., Le Mevel, J. C., Chatenet, D., Tostivint, H., Fournier, A., Tonon, M. C., Pelletier, G., Conlon, J. M., and Leprince, J. (2010) Urotensin II, from fish to human. *Ann. N.Y. Acad. Sci.* **1200,** 53–66
3. Ames, R. S., Sarau, H. M., Chambers, J. K., Willette, R. N., Aiyar, N. V., Romanic, A. M., Louden, C. S., Foley, J. J., Sauermelch, C. F., Coatney, R. W., Ao, Z., Disa, J., Holmes, S. D., Stadel, J. M., Martin, J. D., Liu, W. S., Glover, G. I., Wilson, S., McNulty, D. E., Ellis, C. E., Elshourbagy, N. A., Shabon, U., Trill, J. J., Hay, D. W., Ohlstein, E. H., Bergsma, D. J., and Douglas, S. A. (1999) Human urotensin-II is a potent vasoconstrictor and agonist for the orphan receptor GPR14. *Nature* **401,** 282–286
4. Sainsily, X., Cabana, J., Holleran, B. J., Escher, E., Lavigne, P., and Leduc, R. (2014) Identification of transmembrane domain 1 & 2 residues that contribute to the formation of the ligand-binding pocket of the urotensin-II receptor. *Biochem. Pharmacol.* **92,** 280–288
5. Herold, C. L., Behm, D. J., Buckley, P. T., Foley, J. J., Wixted, W. E., Sarau, H. M., and Douglas, S. A. (2003) The neuromedin B receptor antagonist, BIM-23127, is a potent antagonist at human and rat urotensin-II receptors. *Br. J. Pharmacol.* **139,** 203–207
6. Gartlon, J., Parker, F., Harrison, D. C., Douglas, S. A., Ashmeade, T. E., Riley, G. J., Hughes, Z. A., Taylor, S. G., Munton, R. P., Hagan, J. J., Hunter, J. A., and Jones, D. N. (2001) Central effects of urotensin-II following ICV administration in rats. *Psychopharmacology* **155,** 426–433

7. Do-Rego, J. C., Chatenet, D., Orta, M. H., Naudin, B., Le Cudennec, C., Leprince, J., Scalbert, E., Vaudry, H., and Costentin, J. (2005) Behavioral effects of urotensin-II centrally administered in mice. *Psychopharmacology* **183,** 103–117
8. Huitron-Resendiz, S., Kristensen, M. P., Sánchez-Alavez, M., Clark, S. D., Grupke, S. L., Tyler, C., Suzuki, C., Nothacker, H. P., Civelli, O., Criado, J. R., Henriksen, S. J., Leonard, C. S., and de Lecea, L. (2005) Urotensin II modulates rapid eye movement sleep through activation of brainstem cholinergic neurons. *J. Neurosci.* **25,** 5465–5474
9. Russell, F. D., Molenaar, P., and O'Brien, D. M. (2001) Cardiostimulant effects of urotensin-II in human heart *in vitro*. *Br. J. Pharmacol.* **132,** 5–9
10. Douglas, S. A., Tayara, L., Ohlstein, E. H., Halawa, N., and Giaid, A. (2002) Congestive heart failure and expression of myocardial urotensin II. *Lancet* **359,** 1990–1997
11. Lin, Y., Tsuchihashi, T., Matsumura, K., Fukuhara, M., Ohya, Y., Fujii, K., and Iida, M. (2003) Central cardiovascular action of urotensin II in spontaneously hypertensive rats. *Hypertens. Res.* **26,** 839–845
12. Ng, L. L., Loke, I., O'Brien, R. J., Squire, I. B., and Davies, J. E. (2002) Plasma urotensin in human systolic heart failure. *Circulation* **106,** 2877–2880
13. Bousette, N., and Giaid, A. (2006) Urotensin-II and cardiovascular diseases. *Curr. Hypertens. Rep.* **8,** 479–483
14. Richards, A. M., and Charles, C. (2004) Urotensin II in the cardiovascular system. *Peptides* **25,** 1795–1802
15. Hofmann, F., Flockerzi, V., Kahl, S., and Wegener, J. W. (2014) L-type CaV1.2 calcium channels: from *in vitro* findings to *in vivo* function. *Physiol. Rev.* **94,** 303–326
16. Irisawa, H., Brown, H. F., and Giles, W. (1993) Cardiac pacemaking in the sinoatrial node. *Physiol. Rev.* **73,** 197–227
17. Bers, D. M. (2008) Calcium cycling and signaling in cardiac myocytes. *Annu. Rev. Physiol.* **70,** 23–49
18. Sirenko, S., Yang, D., Li, Y., Lyashkov, A. E., Lukyanenko, Y. O., Lakatta, E. G., and Vinogradova, T. M. (2013) Ca^{2+}-dependent phosphorylation of Ca^{2+} cycling proteins generates robust rhythmic local Ca^{2+} releases in cardiac pacemaker cells. *Sci. Signal.* **6,** ra6
19. Kho, C., Lee, A., and Hajjar, R. J. (2012) Altered sarcoplasmic reticulum calcium cycling—targets for heart failure therapy. *Nat. Rev. Cardiol.* **9,** 717–733
20. Shaw, R. M., and Colecraft, H. M. (2013) L-type calcium channel targeting and local signalling in cardiac myocytes. *Cardiovasc. Res.* **98,** 177–186
21. Wang, X., Boyken, S. E., Hu, J., Xu, X., Rimer, R. P., Shea, M. A., Shaw, A. S., Andreotti, A. H., and Huang, Y. H. (2014) Calmodulin and PI(3,4,5)P3 cooperatively bind to the Itk pleckstrin homology domain to promote efficient calcium signaling and IL-17A production. *Sci. Signal.* **7,** ra74
22. Catterall, W. A. (2000) Structure and regulation of voltage-gated Ca^{2+} channels. *Annu. Rev. Cell Dev. Biol.* **16,** 521–555
23. Tao, J., Hildebrand, M. E., Liao, P., Liang, M. C., Tan, G., Li, S., Snutch, T. P., and Soong, T. W. (2008) Activation of corticotropin-releasing factor receptor 1 selectively inhibits CaV3.2 T-type calcium channels. *Mol. Pharmacol.* **73,** 1596–1609
24. Ferreira, J. C., Boer, B. N., Grinberg, M., Brum, P. C., and Mochly-Rosen, D. (2012) Protein quality control disruption by PKCβII in heart failure; rescue by the selective PKCβII inhibitor, βIIV5-3. *PLoS One* **7,** e33175
25. Stebbins, E. G., and Mochly-Rosen, D. (2001) Binding specificity for RACK1 resides in the V5 region of β II protein kinase C. *J. Biol. Chem.* **276,** 29644–29650
26. Tao, J., Xu, H., Yang, C., Liu, C. N., and Li, S. (2004) Effect of urocortin on L-type calcium currents in adult rat ventricular myocytes. *Pharmacol. Res.* **50,** 471–476
27. Jian, Z., Han, H., Zhang, T., Puglisi, J., Izu, L. T., Shaw, J. A., Onofiok, E., Erickson, J. R., Chen, Y. J., Horvath, B., Shimkunas, R., Xiao, W., Li, Y., Pan, T., Chan, J., Banyasz, T., Tardiff, J. C., Chiamvimonvat, N., Bers, D. M., Lam, K. S., and Chen-Izu, Y. (2014) Mechanochemotransduction during cardiomyocyte contraction is mediated by localized nitric oxide signaling. *Sci. Signal* **7,** ra27
28. Sardesai, N., Lee, L. Y., Chen, H., Yi, H., Olbricht, G. R., Stirnberg, A., Jeffries, J., Xiong, K., Doerge, R. W., and Gelvin, S. B. (2013) Cytokinins secreted by *Agrobacterium* promote transformation by repressing a plant myb transcription factor. *Sci. Signal.* **6,** ra100
29. Kotla, S., Singh, N. K., Heckle, M. R., Tigyi, G. J., and Rao, G. N. (2013) The transcription factor CREB enhances interleukin-17A production and inflammation in a mouse model of atherosclerosis. *Sci. Signal.* **6,** ra83
30. Zhang, Y., Jiang, D., Zhang, Y., Jiang, X., Wang, F., and Tao, J. (2012) Neuromedin U type 1 receptor stimulation of A-type K^+ current requires the $\beta\gamma$ subunits of G_o protein, protein kinase A, and extracellular signal-regulated kinase 1/2 (ERK1/2) in sensory neurons. *J. Biol. Chem.* **287,** 18562–18572
31. Wang, H., Qin, J., Gong, S., Feng, B., Zhang, Y., and Tao, J. (2014) Insulin-like growth factor-1 receptor-mediated inhibition of A-type K^+ current induces sensory neuronal hyperexcitability through the phosphatidylinositol 3-kinase and extracellular signal-regulated kinase 1/2 pathways, independently of Akt. *Endocrinology* **155,** 168–179
32. Russell, F. D. (2008) Urotensin II in cardiovascular regulation. *Vasc. Health Risk Manag.* **4,** 775–785
33. Er, E. E., Mendoza, M. C., Mackey, A. M., Rameh, L. E., and Blenis, J. (2013) AKT facilitates EGFR trafficking and degradation by phosphorylating and activating PIKfyve. *Sci. Signal.* **6,** ra45
34. Niepel, M., Hafner, M., Pace, E. A., Chung, M., Chai, D. H., Zhou, L., Schoeberl, B., and Sorger, P. K. (2013) Profiles of basal and stimulated receptor signaling networks predict drug response in breast cancer lines. *Sci. Signal.* **6,** ra84
35. Niederst, M. J., and Engelman, J. A. (2013) Bypass mechanisms of resistance to receptor tyrosine kinase inhibition in lung cancer. *Sci. Signal.* **6,** re6
36. Blumenstein, Y., Kanevsky, N., Sahar, G., Barzilai, R., Ivanina, T., and Dascal, N. (2002) A novel long N-terminal isoform of human L-type Ca^{2+} channel is up-regulated by protein kinase C. *J. Biol. Chem.* **277,** 3419–3423
37. Viard, P., Macrez, N., Mironneau, C., and Mironneau, J. (2001) Involvement of both G protein αs and $\beta\gamma$ subunits in β-adrenergic stimulation of vascular L-type Ca^{2+} channels. *Br. J. Pharmacol.* **132,** 669–676
38. Pérez-Garci, E., Larkum, M. E., and Nevian, T. (2013) Inhibition of dendritic Ca^{2+} spikes by GABAB receptors in cortical pyramidal neurons is mediated by a direct $G_{i/o}$-β-subunit interaction with Cav1 channels. *J. Physiol.* **591,** 1599–1612
39. Ivanina, T., Blumenstein, Y., Shistik, E., Barzilai, R., and Dascal, N. (2000) Modulation of L-type Ca^{2+} channels by G$\beta\gamma$ and calmodulin via interactions with N and C termini of α1C. *J. Biol. Chem.* **275,** 39846–39854
40. Zhang, H. Y., Liao, P., Wang, J. J., Yu de, J., and Soong, T. W. (2010) Alternative splicing modulates diltiazem sensitivity of cardiac and vascular smooth muscle $Ca_v1.2$ calcium channels. *Br. J. Pharmacol.* **160,** 1631–1640
41. Liao, P., Yu, D., Li, G., Yong, T. F., Soon, J. L., Chua, Y. L., and Soong, T. W. (2007) A smooth muscle Cav1.2 calcium channel splice variant underlies hyperpolarized window current and enhanced state-dependent inhibition by nifedipine. *J. Biol. Chem.* **282,** 35133–35142
42. Hu, C., Depuy, S. D., Yao, J., McIntire, W. E., and Barrett, P. Q. (2009) Protein kinase A activity controls the regulation of T-type CaV3.2 channels by G$\beta\gamma$ dimers. *J. Biol. Chem.* **284,** 7465–7473
43. Zhang, Y., Jiang, D., Zhang, J., Wang, F., Jiang, X., and Tao, J. (2010) Activation of neuromedin U type 1 receptor inhibits L-type Ca^{2+} channel currents via phosphatidylinositol 3-kinase-dependent protein kinase C epsilon pathway in mouse hippocampal neurons. *Cell. Signal.* **22,** 1660–1668
44. Kamp, T. J., and Hell, J. W. (2000) Regulation of cardiac L-type calcium channels by protein kinase A and protein kinase C. *Circ. Res.* **87,** 1095–1102
45. Hoddah, H., Marcantoni, A., Comunanza, V., Carabelli, V., and Carbone, E. (2009) L-type channel inhibition by CB1 cannabinoid receptors is mediated by PTX-sensitive G proteins and cAMP/PKA in GT1–7 hypothalamic neurons. *Cell Calcium* **46,** 303–312
46. Gui, P., Wu, X., Ling, S., Stotz, S. C., Winkfein, R. J., Wilson, E., Davis, G. E., Braun, A. P., Zamponi, G. W., and Davis, M. J. (2006) Integrin receptor activation triggers converging regulation of Cav1.2 calcium channels by c-Src and protein kinase A pathways. *J. Biol. Chem.* **281,** 14015–14025
47. Viard, P., Exner, T., Maier, U., Mironneau, J., Nürnberg, B., and Macrez, N. (1999) G$\beta\gamma$ dimers stimulate vascular L-type Ca^{2+} channels via phosphoi-

nositide 3-kinase. *FASEB J.* **13,** 685–694
48. Bonneau, B., Nougarède, A., Prudent, J., Popgeorgiev, N., Peyriéras, N., Rimokh, R., and Gillet, G. (2014) The Bcl-2 homolog Nrz inhibits binding of IP3 to its receptor to control calcium signaling during zebrafish epiboly. *Sci. Signal.* **7,** ra14
49. Tao, J. J., Castel, P., Radosevic-Robin, N., Elkabets, M., Auricchio, N., Aceto, N., Weitsman, G., Barber, P., Vojnovic, B., Ellis, H., Morse, N., Viola-Villegas, N. T., Bosch, A., Juric, D., Hazra, S., Singh, S., Kim, P., Bergamaschi, A., Maheswaran, S., Ng, T., Penault-Llorca, F., Lewis, J. S., Carey, L. A., Perou, C. M., Baselga, J., and Scaltriti, M. (2014) Antagonism of EGFR and HER3 enhances the response to inhibitors of the PI3K-Akt pathway in triple-negative breast cancer. *Sci. Signal.* **7,** ra29
50. Callaghan, B., Koh, S. D., and Keef, K. D. (2004) Muscarinic M2 receptor stimulation of Cav1.2b requires phosphatidylinositol 3-kinase, protein kinase C, and c-Src. *Circ. Res.* **94,** 626–633
51. Diaz-Flores, E., Goldschmidt, H., Depeille, P., Ng, V., Akutagawa, J., Krisman, K., Crone, M., Burgess, M. R., Williams, O., Houseman, B., Shokat, K., Sampath, D., Bollag, G., Roose, J. P., Braun, B. S., and Shannon, K. (2013) PLC-γ and PI3K link cytokines to ERK activation in hematopoietic cells with normal and oncogenic Kras. *Sci. Signal.* **6,** ra105
52. Chen, S., Jiang, X., Gewinner, C. A., Asara, J. M., Simon, N. I., Cai, C., Cantley, L. C., and Balk, S. P. (2013) Tyrosine kinase BMX phosphorylates phosphotyrosine-primed motif mediating the activation of multiple receptor tyrosine kinases. *Sci. Signal.* **6,** ra40
53. Mohan, M. L., Jha, B. K., Gupta, M. K., Vasudevan, N. T., Martelli, E. E., Mosinski, J. D., and Naga Prasad, S. V. (2013) Phosphoinositide 3-kinase γ inhibits cardiac GSK-3 independently of Akt. *Sci. Signal.* **6,** ra4
54. Wang, Y. X., Dhulipala, P. D., Li, L., Benovic, J. L., and Kotlikoff, M. I. (1999) Coupling of M2 muscarinic receptors to membrane ion channels via phosphoinositide 3-kinase gamma and atypical protein kinase C. *J. Biol. Chem.* **274,** 13859–13864
55. Kusne, Y., Carrera-Silva, E. A., Perry, A. S., Rushing, E. J., Mandell, E. K., Dietrich, J. D., Errasti, A. E., Gibbs, D., Berens, M. E., Loftus, J. C., Hulme, C., Yang, W., Lu, Z., Aldape, K., Sanai, N., Rothlin, C. V., and Ghosh, S. (2014) Targeting aPKC disables oncogenic signaling by both the EGFR and the proinflammatory cytokine TNFα in glioblastoma. *Sci. Signal.* **7,** ra75
56. Alden, K. J., Goldspink, P. H., Ruch, S. W., Buttrick, P. M., and García, J. (2002) Enhancement of L-type Ca^{2+} current from neonatal mouse ventricular myocytes by constitutively active PKC-βII. *Am. J. Physiol. Cell Physiol.* **282,** C768–C774
57. Yang, L., Liu, G., Zakharov, S. I., Morrow, J. P., Rybin, V. O., Steinberg, S. F., and Marx, S. O. (2005) Ser^{1928} is a common site for Cav1.2 phosphorylation by protein kinase C isoforms. *J. Biol. Chem.* **280,** 207–214
58. Zhang, Z. H., Johnson, J. A., Chen, L., El-Sherif, N., Mochly-Rosen, D., and Boutjdir, M. (1997) C2 region-derived peptides of β-protein kinase C regulate cardiac Ca^{2+} channels. *Circ. Res.* **80,** 720–729
59. El Khoury, N., Mathieu, S., and Fiset, C. (2014) Interleukin-1β reduces L-type Ca^{2+} current through protein kinase C activation in mouse heart. *J. Biol. Chem.* **289,** 21896–21908
60. Wu, B. N., Chen, M. L., Dai, Z. K., Lin, Y. L., Yeh, J. L., Wu, J. R., and Chen, I. J. (2009) Inhibition of voltage-gated L-type calcium channels by labedipinedilol-A involves protein kinase C in rat cerebrovascular smooth muscle cells. *Vascul. Pharmacol.* **51,** 65–71
61. Tseng, G. N., and Boyden, P. A. (1991) Different effects of intracellular Ca and protein kinase C on cardiac T and L Ca currents. *Am. J. Physiol. Heart Circ. Physiol.* **261,** H364–H379
62. Walsh, K. B., and Kass, R. S. (1988) Regulation of a heart potassium channel by protein kinase A and C. *Science* **242,** 67–69
63. Dempsey, E. C., Newton, A. C., Mochly-Rosen, D., Fields, A. P., Reyland, M. E., Insel, P. A., and Messing, R. O. (2000) Protein kinase C isozymes and the regulation of diverse cell responses. *Am. J. Physiol. Lung Cell. Mol. Physiol.* **279,** L429–L438
64. Sonkusare, S. K., Dalsgaard, T., Bonev, A. D., Hill-Eubanks, D. C., Kotlikoff, M. I., Scott, J. D., Santana, L. F., and Nelson, M. T. (2014) AKAP150-dependent cooperative TRPV4 channel gating is central to endothelium-dependent vasodilation and is disrupted in hypertension. *Sci. Signal.* **7,** ra66
65. Maeno-Hikichi, Y., Chang, S., Matsumura, K., Lai, M., Lin, H., Nakagawa, N., Kuroda, S., and Zhang, J. F. (2003) A PKCϵ-ENH-channel complex specifically modulates N-type Ca^{2+} channels. *Nat. Neurosci.* **6,** 468–475
66. Poole, A. W., Pula, G., Hers, I., Crosby, D., and Jones, M. L. (2004) PKC-interacting proteins: from function to pharmacology. *Trends Pharmacol. Sci.* **25,** 528–535
67. Farren, M. R., Carlson, L. M., Netherby, C. S., Lindner, I., Li, P. K., Gabrilovich, D. I., Abrams, S. I., and Lee, K. P. (2014) Tumor-induced STAT3 signaling in myeloid cells impairs dendritic cell generation by decreasing PKCβII abundance. *Sci. Signal.* **7,** ra16
68. Liao, P., Yu, D., Lu, S., Tang, Z., Liang, M. C., Zeng, S., Lin, W., and Soong, T. W. (2004) Smooth muscle-selective alternatively spliced exon generates functional variation in Cav1.2 calcium channels. *J. Biol. Chem.* **279,** 50329–50335
69. Lao, Q. Z., Kobrinsky, E., Harry, J. B., Ravindran, A., and Soldatov, N. M. (2008) New determinant for the CaVβ2 subunit modulation of the CaV1.2 calcium channel. *J. Biol. Chem.* **283,** 15577–15588